Magnetic Circular Dichroism of the Iron(III) Porphins

Hiroshi Kobayashi, Tadatoshi Higuchi, and Ken Eguchi

Department of Chemistry, Tokyo Institute of Technology, Ookayama, Meguro-ku, Tokyo 152

(Received July 5, 1975)

Magnetic circular dichroism(MCD) spectra were measured of some low-spin and high-spin Fe(III) porphins in a rigid matrix of polymethyl methacrylate(PMMA) for a variety of temperature. Some of the most prominent MCD extrema of the low-spin Fe(III) porphins showed a remarkable enhancement of the intensity at reduced temperatures, while no appreciable increase was observed in the absorption intensity. The temperature dependence of the MCD dispersion of the low-spin Fe(III) porphins arises, in principle, from a change in the Boltzmann distribution between the ground Kramers doublet splitting in a magnetic field, however, the MCD enhancement observed in the Soret region can correctly be interpreted only when the excited states described by a product wave function of the porphin B state and the spin-orbit coupling substates of low-spin iron(III) d^5 system are split by a configuration interaction with the "porphin to iron(III)" charge-transfer excited states.

The visible and near-ultraviolet absorption spectra of metalloporphyrins arise from the lowest spin-allowed (π, π^*) excitations.[1-3] The role of the central metal ion in the absorption spectra is of relatively minor in most metalloporphyrins, whereas the lifetime of the excited metalloporphyrins depends upon the structure of interactions between the π-electron system of porphyrin and the central transition metal ion.[4-9] In some metalloporphyrins with $d\pi$-open shell such as high-spin iron(III) porphyrins and high-spin manganese(III) porphyrins, a participation of "porphyrin to metal" charge-transfer (CT) excited states in the lowest electronic excited states gives rise to an observable anomaly in the absorption spectra.[10]

The temperature-dependent *C*-term extrema in the (π, π^*) transitions of the ligand coordinated to a metal ion in a degenerate ground state should be observed only when an appreciable interaction between the π-electron system of the ligand and the open-shell orbital of the central metal ion is present. In this paper, a study of temperature changes of the MCD spectra in the lowest excitations of the iron(III) porphyrins is presented.

Experimental

Synthesis of the Metal-free Base of Tetraphenylporphin (H_2TPP). H_2TPP was synthesized by the method of Adler *et al.*[11] Chromatographic purification was repeated on activated alumina columns using chloroform as solvent and also as eluent. The elute was concentrated, and then excess methanol was added. Purple needle crystals thus obtained were identified by elemental analysis.

Found: C, 86.18; H, 4.61; N, 8.96%. Calcd for $C_{44}H_{30}N_4$: C, 85.97; H, 4.92; N, 9.11%.

Synthesis of Tetraphenylporphinatoiron(III) Chloride (TPPFe(III)Cl). TPPFe(III)Cl was prepared in dimethylformamide (DMF). H_2TPP (0.3 g) and $FeCl_2\cdot 4H_2O$ (1.5 g) were dissolved in DMF (200 ml) and refluxed for 3 hr. When the solution was cooled, portions of dilute hydrochloric acid were added by a small amount. The dark purple crystals thus precipitated were collected by filteration. The complex was recrystallized twice from a mixture of 1,2-dichloroethane and hexane.

Found: C, 74.94; H, 3.85; N, 7.92; Fe, 7.97; Cl, 5.10%. Calcd for $C_{44}H_{28}N_4FeCl$: C, 75.07; H, 4.01; N, 7.96; Fe, 7.93; Cl, 5.04%.

Synthesis of Bisimidazoletetraphenylporphinatoiron(III) Perchlorate ([TPPFe(III)(Im)$_2$]ClO$_4$). TPPFe(III)Cl (35 mg) was dissolved in benzene (5 ml). $AgClO_4$ (10 mg) was added to the solution. After reflux for 4 hr, AgCl was filtered off and then imidazole (6 mg) was added. Just after the addition of imidazole, reddish purple crystals precipitated. When the precipitation was completed, unreacted $AgClO_4$ and imidazole were dissolved by adding ethyl ether (5 ml). The residue was dissolved in 1,2-dichloroethane and then filtered for separation of the contaminating $AgClO_4$. The filtrate was condensed under reduced pressure and then benzene was added to it for precipitation. Pure crystals were obtained by recrystallization from a mixture of 1,2-dichloroethane and benzene.

Found: C, 66.18; H, 3.67; N, 12.50; Fe, 6.08%. Calcd for $C_{50}H_{36}N_8FeClO_4$: C, 66.42; H, 4.01; N, 12.39; Fe, 6.18%.

Synthesis of the Metal-free Bases of Octaethylporphin (H_2OEP). H_2OEP was prepared by refluxing 3,4-diethyl-5-hydroxymethylpyrrole-2-carboxylic acid and potassium ferricyanide in glacial acetic acid according to the method of Inhoffen *et al.*[12] Octaethylporphin thus obtained was recrystallized from a mixture of chloroform and methanol and purified by column chromatography.

Found: C, 80.55; H, 8.51; N, 10.44%. Calcd for $C_{36}H_{46}N_4$: C, 80.85; H, 8.67; N, 10.48%.

Synthesis of Octaethylporphinatoiron(III) Chloride (OEPFe(III)Cl). OEPFe(III)Cl was prepared by a method similar to the preparation of TPPFe(III)Cl. H_2OEP (250 mg) was dissolved in refluxing dimethylformamide (100 ml). $FeCl_2\cdot 4H_2O$ (1.5 g) was added to the refluxing solution of the free base. After reflux for 3 hr, portions of dilute hydrochloric acid were added by a small amount when the refluxed solution was cooled. The product was recrystallized twice from a mixture of 1,2-dichloroethane and hexane.

Found: C, 68.60; H, 6.88; N, 9.16; Fe, 8.55; Cl, 6.00%. Calcd for $C_{36}H_{44}N_4FeCl$: C, 69.29; H, 7.11; N, 8.98; Fe, 8.95; Cl, 5.68%.

Synthesis of Bisimidazoleoctaethylporphinatoiron(III) Perchlorate ([OEPFe(III)(Im)$_2$]ClO$_4$). [OEPFe(III)(Im)$_2$]ClO$_4$ was prepared by the method of Ogoshi *et al.*[13] OEPFe(III)Cl (150 mg) was dissolved in benzene (50 ml), and $AgClO_4$ (200 mg) was added. The reaction mixture was refluxed for 3 hr. After imidazole (80 mg) dissolved in benzene (15 ml) was added, the reaction mixture was refluxed continuously until the solution became transparent. The precipitates were separated by filteration, and extracted with 1,2-dichloroethane. Crude crystals were obtained by removing the solvent under reduced pressure. Dark brown pure crystals were obtained by recrystallization from a mixture of 1,2-dichloroethane and benzene.

Other metal porphins TPPMn(III)Cl, TPPCo(II), and TPPZn(II) used in the present measurements were prepared in our previous works[10,14,15] and used without further purification.

Measurements of Absorption and Magnetic Circular Dichroism Spectra. The electronic absorption spectra were recorded on a Shimadzu recording spectrophotometer Model MPS-50. Solvents were benzene and 1,2-dichloroethane purified by fractional distillation using a 1.5 m Dixson-ring packed column and dried by the usual procedure.[16]

The circular dichroism under an external magnetic field (MCD) was measured by a JASCO automatic recording spectropolarimeter Model ORD/UV-5 with its CD attachment and electromagnet. The magnetic field was set at 10000 gauss.

A cryostat was adopted for measurements of the spectra at liquid-nitrogen temperature and dry ice-methanol temperature. For the low-temperature measurements, the porphins were dispersed in an appropriate polymer film. In the case of TPPFe(III)Cl, OEPFe(III)Cl, [TPPFe(III)-(Im)$_2$]ClO$_4$, [OEPFe(III)(Im)$_2$]ClO$_4$, TPPMn(III)Cl, and TPPZn(II), polymethyl methacrylate was used for matrices. By spontaneous evaporation of a viscous solution, which was obtained by dissolving polymethyl methacrylate and porphin in 1,2-dichloroethane, a transparent film dispersing porphin was prepared on a clean glass plate. In the case of TPPFe-(III)Cl and TPPZn, polystyrene was also used. A polystyrene film was made on a glass plate by spontaneous evaporation of a viscous solution, which was obtained by dissolving polystyrene and porphin in 1,2-dichloroethane. After evacuation, the film was melted in a glass tube at about 200 °C under nitrogen atmosphere which was used for polystyrene not to be oxidized. The bubbles in polystyrene were eliminated by recycling evacuation of the atmosphere in the glass tube and introduction of nitrogen gas. The polystyrene gave a rigid glass without cracks and distortion when slowly cooled. The sample was cut in a disk and its faces were polished so as to make optical measurements possible. Since TPPCo(II) might be oxidized during preparation of the rigid glass sample, TPPCo(II) was directly fused in polystyrene under nitrogen atmosphere.

ESR Spectra. The ESR spectra were obtained by a Japan Electron Optics Laboratory spectrometer Model JES ME3X. The static magnetic field was calibrated by means of a proton-resonance gaussmeter.

Results and Discussion

The MCD spectra of TPPFe(III)Cl and OEPFe-(III)Cl, which are typical iron(III) porphins in the high spin state $S=5/2$, were observed in benzene. The results are presented in Figs. 1 and 2. The similar spectra were obtained in polystyrene. Quantitative spectrum, however, could not be obtained, since the back-ground absorption of polystyrene increased so fast in the higher wave number region that a reproducible calibration was impossible. In the case of PMMA matrices, reproducible spectra of the porphins were obtained. In fact, the spectra of the rigid polymer glass at room temperature were coincident with the solution spectra. The absorption and MCD spectra of TPPFe(III)Cl and OEPFe(III)Cl in PMMA were measured for a variety of temperature as shown in Figs. 3 and 4.

The MCD spectra of [TPPFe(III)(Im)$_2$]ClO$_4$ and [OEPFe(III)(Im)$_2$]ClO$_4$, which are typical iron(III) porphins in the low spin state $S=1/2$, were observed in C$_2$H$_4$Cl$_2$, and in PMMA for a variety of temperature. The results are presented in Figs. 5, 6, 7, and 8. The similar spectra were also obtained for [TPPFe(III)(Im)$_2$]Cl and [TPPFe(III)(Im)$_2$]ClO$_4$ in chloroform which consists of ten times or more excess imidazole. La Mar and Walker also ob-

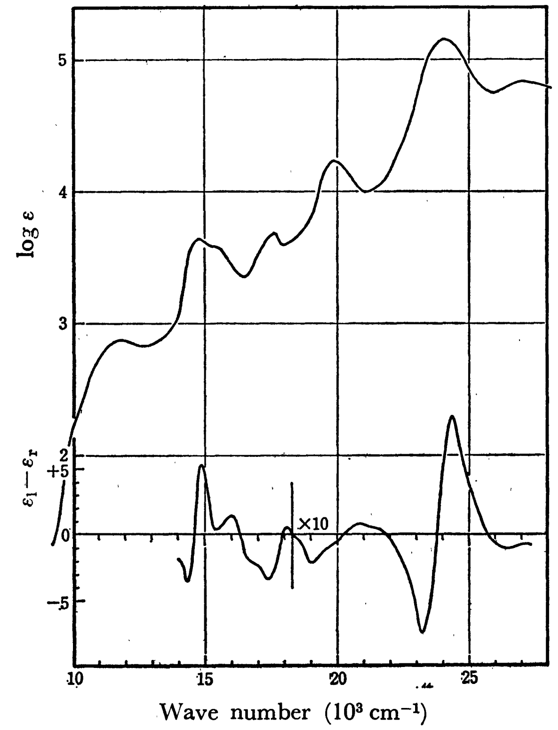

Fig. 1. The absorption and MCD spectra of TPPFe-(III)Cl in C$_6$H$_6$.

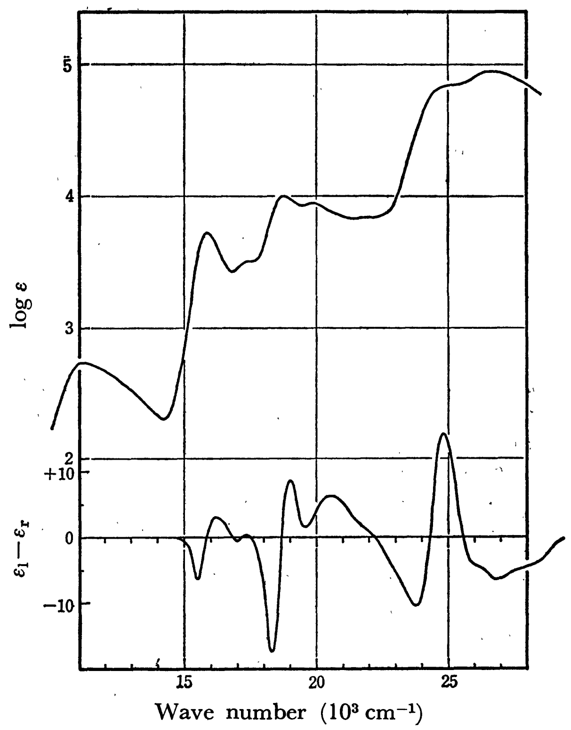

Fig. 2. The absorption and MCD spectra of OEPFe-(III)Cl in C$_6$H$_6$.

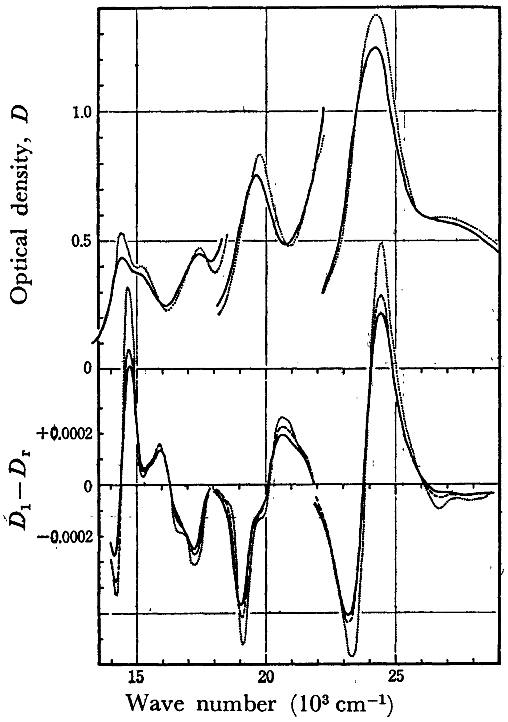

Fig. 3. The absorption and MCD spectra of TPPFe(III)Cl in PMMA.
——: 310 K; - - - -: 196 K; ······: 79 K.

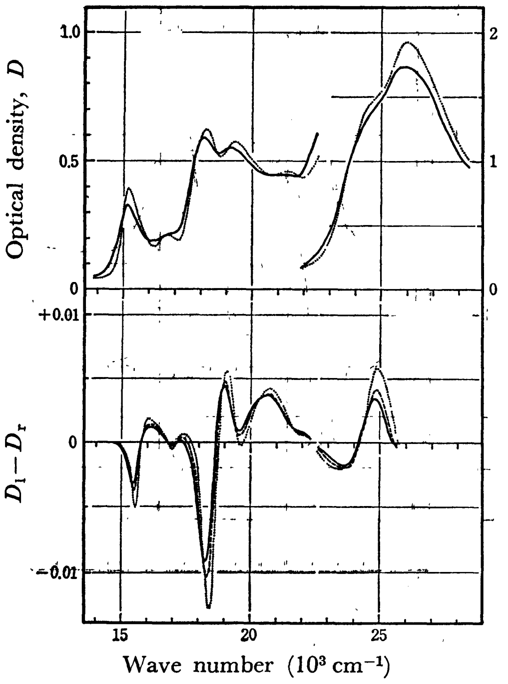

Fig. 4. The absorption and MCD spectra of OEPFe(III)Cl in PMMA. ——: 310 K; - - - -: 196 K; ······: 79 K.

served in their NMR studies that the proton signals of the low-spin species were detected only in the presence of eight times excess imidazole in deutero-chloroform.[17] In chloroform, however, the dissociation of coordinated imidazole gives rise to a drift of the spectrum even in the presence of excess imidazole. In 1,2-dichloroethane, on the other hand, a spectrum characteristic

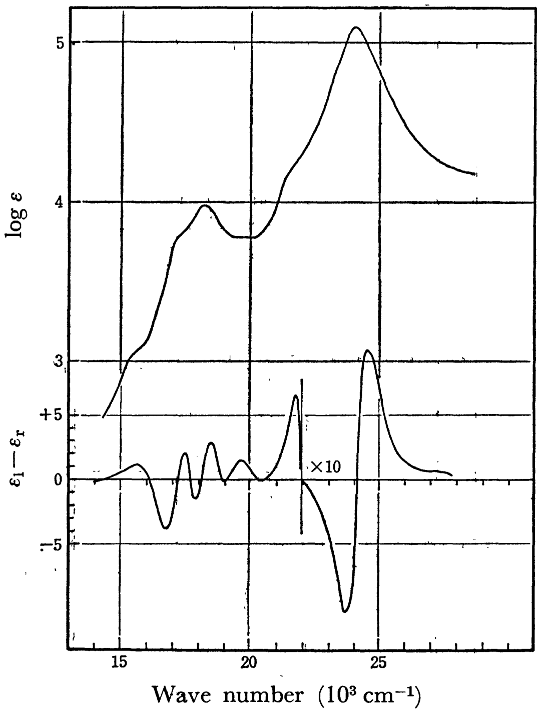

Fig. 5. The absorption and MCD spectra of [TPPFe(III)(Im)$_2$]ClO$_4$ in C$_2$H$_4$Cl$_2$.

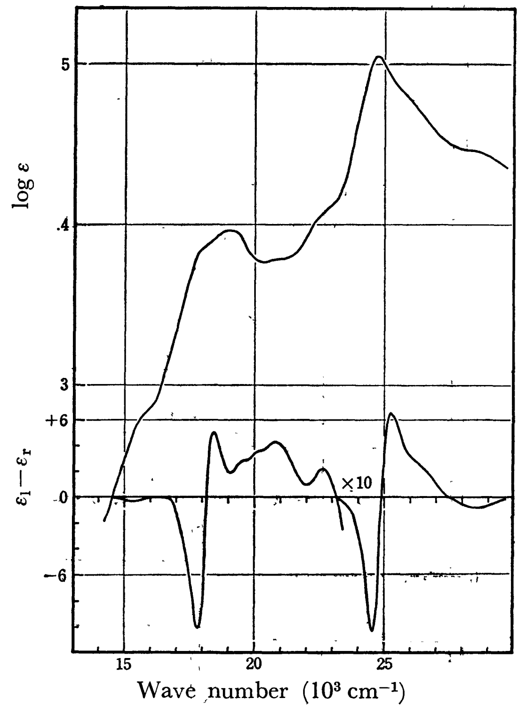

Fig. 6. The absorption and MCD spectra of [OEPFe(III)(Im)$_2$]ClO$_4$ in C$_2$H$_4$Cl$_2$.

of the low-spin iron(III) porphins did not change for a few days after the solid sample was dissolved in the absence of excess imidazole. The spectra obtained for TPPMn(III)Cl in PMMA, TPPCo(II) in polystyrene, and TPPZn(II) in PMMA are also shown in Figs. 9, 10, and 11.

A most remarkable enhancement of MCD extrema was observed in the low-spin iron(III) porphins when

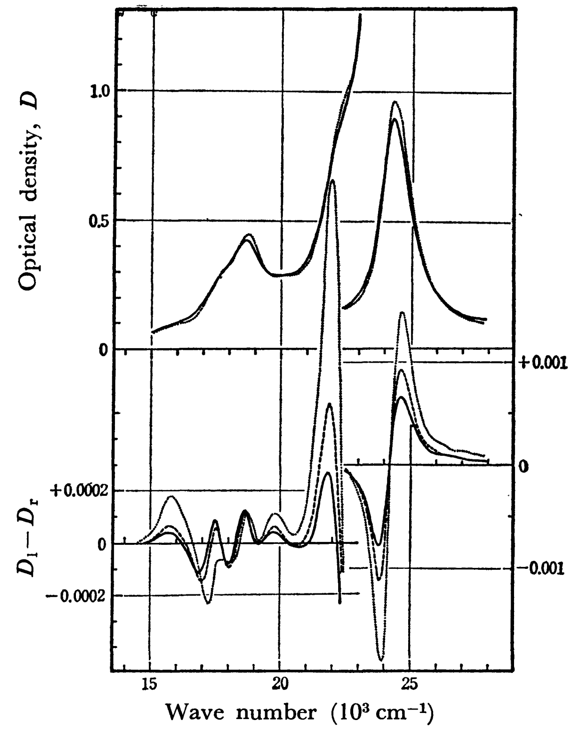

Fig. 7. The absorption and MCD spectra of [TPPFe(III)$(Im)_2$]ClO_4 in PMMA. ——: 310 K; ----: 196 K; ······: 79 K.

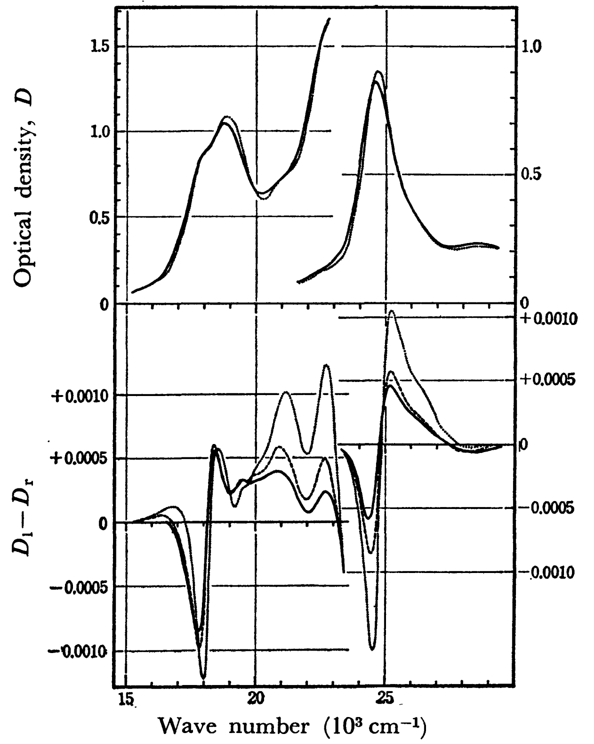

Fig. 8. The absorption and MCD spectra of [OEPFe(III)$(Im)_2$]ClO_4 in PMMA. ——: 310 K; ----: 196 K; ······: 79 K.

the temperature is reduced. At the liquid-nitrogen temperature, two MCD peaks in the lower energy region of the B band increase their intensity up to several times greater than those at room temperature.

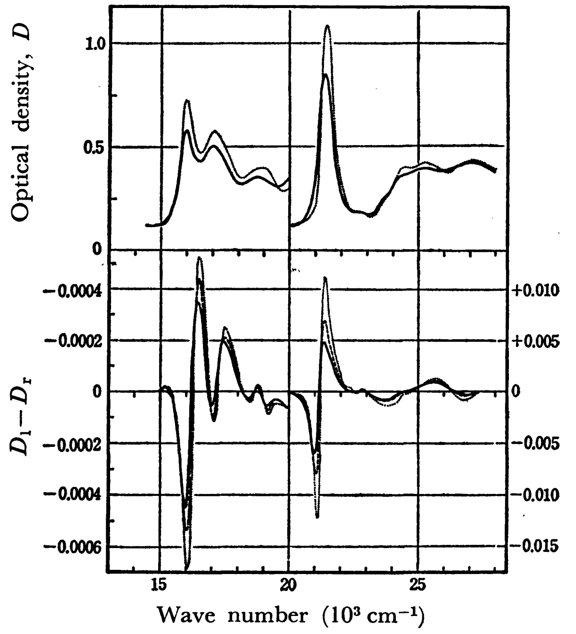

Fig. 9. The absorption and MCD spectra of TPPMn(III)Cl in PMMA. ——: 310 K; ----: 196 K; ······: 79 K.

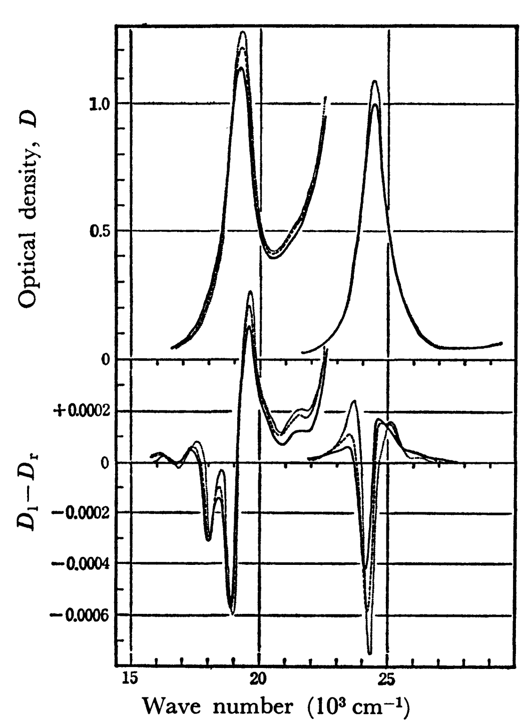

Fig. 10. The absorptioon and MCD spectra of TPPCo(II) in PMMA. ——: 310 K; ---- 196 K; ······: 79 K.

The MCD extrema in the B band also increase their intensity at reduced temperatures. TPPCo(II) and TPPMn(III)Cl also exhibit the similar enhancement.

The absorption band is simulated by a damped oscillator or Gaussian spectral shape function.[18] Supposed that other factors are unchanged, the intensity of *A*-term dispersion extrema is inversely proportional to a square of the line width, while the intensities of *B*-term extrema and of absorption maxima are in-

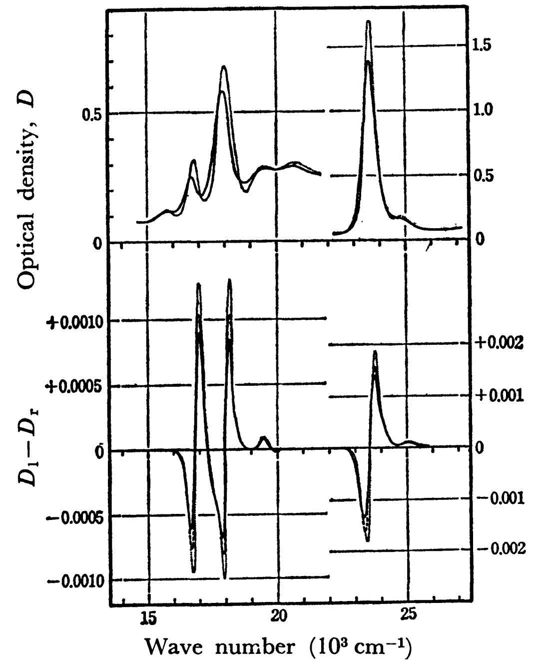

Fig. 11. The absorption and MCD spectra of TPPZn(II) in PMMA. ——: 310 K; ----: 196 K; ……: 79 K.

versely proportional to the line width,

$$\theta^{A}_{\max} \propto (1/\Gamma(T))^2,\ \theta^{B}_{\max} \propto 1/\Gamma(T) \text{ and } \varepsilon^{B}_{\max} \propto 1/\Gamma(T),$$

where Γ is the line width and a function of temperature T. Thus a ratio of the intensities of MCD extrema observed at two different temperatures is correlated with a ratio of the absorption intensities at the corresponding temperatures as follows:

$$\theta^{A}_{\max}(T_2)/\theta^{A}_{\max}(T_1) = \{\varepsilon_{\max}(T_2)/\varepsilon_{\max}(T_1)\}^2$$

and

$$\theta^{B}_{\max}(T_2)/\theta^{B}_{\max}(T_1) = \varepsilon_{\max}(T_2)/\varepsilon_{\max}(T_1).$$

Here it is noted that the ratio R_θ of the intensities of MCD extrema at liquid-nitrogen temperature and at ambient temperature is equal to or less than the square of the corresponding ratio R^2_ε of the absorption maxima. When R_θ is much greater than R^2_ε, a mechanism other than temperature-broadening of the line width should be working. The R_θ's and R^2_ε's observed for the samples studied in the present work are summarized in Fig. 12. The R_θ of TPPZn(II), in which only a small interaction between metal and porphin is present, is in good agreement with its corresponding R^2_ε. This implies that the MCD dispersions observed in the absorption bands of TPPZn(II) are assigned to A-term dispersions. A greater deviation was found in the case of two low-spin iron(III) porphins, TPPCo(II), and TPPMn(III)Cl. Here it is noted that a change of R_θ over the observed wave numbers was analogous in two different low-spin iron(III) porphins.

The ground state of the low-spin iron(III) porphin is described as a composite system of the ground state of porphin π system and the lowest Kramers doublet of low-spin iron d^5 system as follows:

$$A^{+}(+1) = |+4+\bar{4}-4-\bar{4}\,\zeta\,\bar{\zeta}+1+\bar{1}-1|,$$

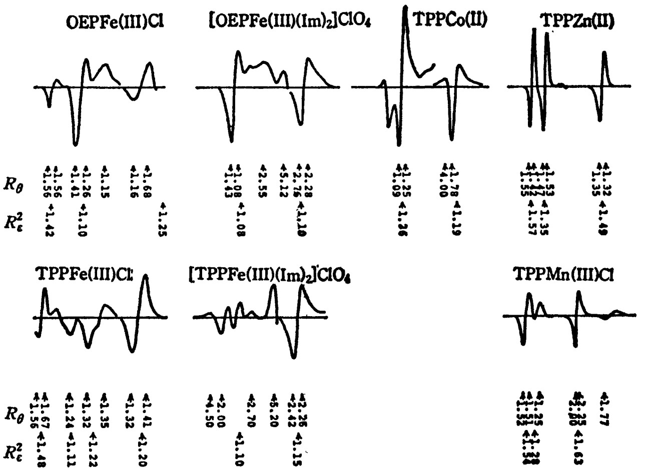

Fig. 12. $R_\theta = \left\{\dfrac{\theta_{\max}(79\text{ K})}{\theta_{\max}(310\text{ K})}\right\}$ and $R_\varepsilon{}^2 = \left\{\dfrac{\varepsilon_{\max}(79\text{ K})}{\varepsilon_{\max}(310\text{ K})}\right\}^2$.

and

$$A^{-}(-1) = |+4+\bar{4}-4-\bar{4}\,\zeta\,\bar{\zeta}-1-\bar{1}+\bar{1}|,$$

where the numbers ±1 given in the parentheses are the orbital angular momenta, the superscripts ± indicate the α- and β-components of the Kramers doublet, ±4 are the highest occupied porphin π orbitals, ζ is iron xy orbital, ±1 are iron $d_{\pm 1}$ orbitals, no bar implies spin α and a bar implies spin β. Thus the spin-allowed excited states of the low-spin iron(III) porphin should be spin-doublets. The composite doublets arise from products of the Kramers doublets of low-spin iron d^5 system and the porphin-localized lowest (π, π^*) excited states, not only of spin-singlet but also of triplet. The doublets given by the product wave funtions of the lowest Kramers' doublet of low-spin iron d^5 system and the porphin-localized Soret excited state B are denoted by $B^{+}(+2)$, $B^{-}(-2)$, $B^{+}(0)$, and $B^{-}(0)$:

$$B^{+}(+2) = \frac{1}{\sqrt{2}}\{|-4-\bar{4}+4+\bar{5}\,\zeta\,\bar{\zeta}+1+\bar{1}-1| - |-4-\bar{4}+\bar{4}+5\,\zeta\,\bar{\zeta}+1+\bar{1}-1|\}$$

$$B^{-}(-2) = \frac{1}{\sqrt{2}}\{|+4+\bar{4}-4-\bar{5}\,\zeta\,\bar{\zeta}-1-\bar{1}+\bar{1}| - |+4+\bar{4}-\bar{4}-5\,\zeta\,\bar{\zeta}-1-\bar{1}+\bar{1}|\}$$

$$B^{+}(0) = \frac{1}{\sqrt{2}}\{|+4+\bar{4}-4-\bar{5}\,\zeta\,\bar{\zeta}+1+\bar{1}-1| - |+4+\bar{4}-\bar{4}-5\,\zeta\,\bar{\zeta}+1+\bar{1}-1|\}$$

$$B^{-}(0) = \frac{1}{\sqrt{2}}\{|-4-\bar{4}+4+\bar{5}\,\zeta\,\bar{\zeta}-1-\bar{1}+\bar{1}| - |-4-\bar{4}+\bar{4}+5\,\zeta\,\bar{\zeta}-1-\bar{1}+\bar{1}|\}$$

Here the numbers given in the parentheses are the orbital angular momenta, the superscripts ± indicate the α- and β-components of the Kramers doublet, and ±5 are the lowest vacant porphin π orbitals. The excitations $A^{+}(+1) \rightarrow B^{+}(+2)$ and $A^{-}(-1) \rightarrow B^{-}(0)$ are left-handed circularly polarized, while the excitations $A^{-}(-1) \rightarrow B^{-}(-2)$ and $A^{+}(+1) \rightarrow B^{+}(0)$ are right-handed circularly polarized. An MCD dispersion occurs in the excitations $A^{+}(+1) \rightarrow B^{+}(+2)$ and $B^{+}(0)$

and also in the excitations $A^-(-1) \rightarrow B^-(-2)$ and $B^-(0)$. When the temperature is reduced, $A^-(-1)$ is more populated than $A^+(+1)$. However no practical change in MCD happens even at reduced temperatures if the B_1 states ($B^+(+2)$ and $B^-(-2)$), in which an orbital angular momentum induced upon excitation is in the direction of the resultant momentum of spin-orbit coupling at the central iron(III) ion, and the B_2 states ($B^+(0)$ and $B^-(0)$), in which an orbital angular momentum induced upon excitation is against the iron momentum, are degenerate.

Since the vacant $d\pi$ orbital and the lowest vacant porphin π^* orbital are equivalent in symmetry and thus, an electron-delocalization is possible between the $d\pi$ and π^* orbitals, the low-energy "porphin to iron(III)" CT excited states exhibit a configuration interaction against the lowest porphin-localized (π, π^*) excited states.[10] A difference in the configuration interactions of the "porphin to iron(III)" CT excited states against the porphin (π, π^*) excited states arises between the B_1 and B_2 states from a difference in symmetry of the doublet eigenfunctions of spin-orbit coupling in the low-spin iron(III) ion embedded in the excited porphin. The $B^+(0)$ and $B^-(0)$ states interact with the CT excited states $CT^+(+4) = |+4+\bar{4}-4\ \zeta\ \bar{\zeta}+1+\bar{1}-1-\bar{1}|$ and $CT^-(-4) = |-4-\bar{4}+\bar{4}\ \zeta\ \bar{\zeta}+1+\bar{1}-1-\bar{1}|$, respectively, while there is no such CT excited states interacting with the $B^+(+2)$ and $B^-(-2)$ states in a first-order approximation.

$$\begin{array}{llcc}
 & & B^+(0) & -CT^+(+4) \\
 & & (B^-(0)) & (CT^-(-4)) \\
\hline
B^+(0) & (B^-(0)) & E+2K_1-\frac{1}{2}a & \frac{\sqrt{2}}{2}X \\
-CT^-(+4) & (CT^-(-4)) & \frac{\sqrt{2}}{2}X & E_{CT}
\end{array}$$

Here $E+2K_1$ and E_{CT} are the diagonal energies of the B state and the CT state, a is the spin-orbit coupling constant and X is the resonance integral between porphin ±5 orbital and iron $d_{\pm 1}$ orbital. Since the "porphin to iron(III)" CT excited states in low-spin iron(III) porphins are lower than the B states,[10] the CT states raise the $B^{\pm}(0)$ states. The empirical values $E = 13070\ \text{cm}^{-1}$, $K_1 = 4600\ \text{cm}^{-1}$, $X = -3000\ \text{cm}^{-1}$ [10] and $a = 435\ \text{cm}^{-1}$ [19] predict an energy gap ΔE between $B^{\pm}(0)$ and $B^{\pm}(\pm 2)$ as a function of E_{CT} as follows:

$E_{CT} = 10000\ \text{cm}^{-1}$ $\Delta E = 360\ \text{cm}^{-1}$
$E_{CT} = 12500\ \text{cm}^{-1}$ $\Delta E = 450\ \text{cm}^{-1}$
$E_{CT} = 15000\ \text{cm}^{-1}$ $\Delta E = 590\ \text{cm}^{-1}$

The mixing of the "porphin to iron(III)" CT excited states to B_1 states occurs to a less extent than the interaction to B_2 states even if in a higher approximation. In fact, the B band of low-spin iron(III) porphins is evidently broad as compared with the B band observed for a typical (π, π^*) transition in TPPZn(II). An MCD dispersion experimentally observed in the Soret region, however, indicates that a gap between the B_1 and B_2 states should be less than the band width ($1000\ \text{cm}^{-1}$) of each component absorption band. Since $A^-(-1)$ is more populated than $A^+(+1)$ at reduced temperatures, the low-energy component transition $A^-(-1) \rightarrow B^+(-2)$ which is right-handed circularly polarized and the high-energy component transition $A^-(-1) \rightarrow B^-(0)$ which is left-handed circularly polarized enhance their absorption intensities. An apparent dispersion is thus obtained by superposing two temperature-dependent C-term extrema with opposite sign for a small energy gap of the excitations to B_1 and B_2 states.

The ESR spectrum of powder $[\text{TPPFe(III)(Im)}_2]\text{ClO}_4$ at 77 K exhibits three different g-values at $g_{zz} = 2.87$, $g_{yy} = 2.26$, and $g_{xx} = 1.65$. The g-values of powder $[\text{TPPFe(III)(Im)}_2]\text{Cl}$ prepared in the present work were $g_{zz} = 2.91$, $g_{yy} = 2.31$, and $g_{xx} = 1.54$ and in good agreement with the values $g_1 = 2.9$, $g_2 = 2.3$, and $g_3 = 1.5$ reported for $[\text{TPPFe(III)(Im)}_2]\text{Cl}$ in a frozen chloroform solution containing excess imidazole.[20] These anisotropic g-values insist that the iron $d_{\pm 1}$ orbitals are split by the π-interaction due to the axial ligands and the lowest Kramers doublet is predominantly made of a degenerate configuration ((xy) $(\overline{xy})$ (zx) $(\overline{zx})$ (yz); (xy) $(\overline{xy})$ (zx) $(\overline{zx})$ $(\overline{yz})$). The lowest component of the spin-orbit coupling sublevels of low-spin d^5 system is about 99.3% occupied even at 300 K.[19] For such a ground state, the arguments similar to those given for the ground state $A^{\pm}(\pm 1)$ can be applicable and predict a temperature-dependent MCD dispersion. As revealed by X-ray studies, two coordinated imidazole molecules are in almost coplanar in the crystal.[21,22] However an internal rotation of the coordinated imidazoles is not so hindered in solution and then the anisotropy becomes smaller than expected from three g-values observed for the solid sample.

In the course of the present work, an independent observation on the temperature-dependent MCD spectra of the low-spin iron(III) porphyrins in hemoproteins was informed the authors before its publication by Dr. T. Nozawa, Tohoku University. The authors' thanks are due to Dr. H. Ogoshi, Kyoto University, for his advice concerning the preparation of porphyrinato-iron(III) perchlorates. The authors are also indebted to Professor J. Higuchi and Dr. T. Ito for the measurements of ESR spectra.

References

1) M. Gouterman, *J. Chem. Phys.*, **30**, 1139 (1959).
2) H. Kobayashi, *ibid.*, **30**, 1362 (1959).
3) C. Weiss, H. Kobayashi, and M. Gouterman, *J. Mol. Spectrosc.*, **16**, 415 (1965).
4) B. E. Smith and M. Gouterman, *Chem. Phys. Lett.*, **2**, 517 (1968).
5) D. Eastwood and M. Gouterman, *J. Mol. Spectrosc.*, **30**, 437 (1969).
6) R. L. Ake and M. Gouterman, *Theoret. Chim. Acta* (Berl.), **15**, 20 (1969).
7) R. L. Ake and M. Gouterman, *ibid.*, **17**, 408 (1970).
8) M. Gouterman, R. A. Mathies, B. E. Smith, and W. S. Caughey, *J. Chem. Phys.*, **52**, 3795 (1970).
9) J. Bohandy, B. F. Kim, and C. K. Jen, *J. Mol. Spectrosc.*, **49**, 365 (1974).
10) H. Kobayashi, Y. Yanagawa, H. Osada, S. Minami,

and M. Shimizu, This Bulletin, **46**, 1471 (1973).

11) A. D. Adler, F. R. Longo, J. D. Finarelli, J. Goldmacher, J. Assour, and L. Korsakoff, *J. Org. Chem.*, **32**, 476 (1967).

12) H. H. Inhoffen, J. H. Fuhrhop, H. Voigt, and H. Brockmann, Jr., *Ann. Chem.*, **695**, 133 (1966).

13) H. Ogoshi, E. Watanabe, Z. Yoshida, J. Kincaid, and K. Nakamoto, *J. Amer. Chem. Soc.*, **95**, 2845 (1973).

14) H. Kobayashi, M. Shimizu, and I. Fujita, This Bulletin, **43**, 2335 (1970).

15) H. Kobayashi, T. Hara, and Y. Kaizu, *ibid.*, **45**, 2148 (1972).

16) D. D. Perrin, W. L. F. Armarego, and D. R. Perrin, "Purification of Laboratory Chemicals," Pergamon Press, Oxford (1966).

17) G. N. La Mar and F. A. Walker, *J. Amer. Chem. Soc.*, **94**, 8607 (1972).

18) P. J. Stephens, W. Suëtaka, and P. N. Schatz, *J. Chem. Phys.*, **44**, 4592 (1966).

19) M. Kotani, *Progr. Theoret. Phys. Suppl.*, **17**, 4 (1961).

20) G. N. La Mar and F. A. Walker, *J. Amer. Chem. Soc.*, **95**, 1782 (1973).

21) D. M. Collins, R. Countryman, and J. L. Hoard, *ibid.*, **87**, 2312 (1965).

22) A. Takenaka, Y. Sadasa, E. Watanabe, H. Ogoshi, and Z. Yoshida, *Chem. Lett.*, **1972**, 1235.